Progress of Theoretical Physics, Vol. 64, No. 5, November 1980

Nucleus-Nucleus Interaction and Nuclear Saturation Property

——*Microscopic Study of* $^{16}O+^{16}O$ *Interaction by New Effective Nuclear Force*——

Tomoaki ANDO, Kiyomi IKEDA* and Akihiro TOHSAKI-SUZUKI**

Fuyo Data Processing and Systems Development Ltd., Minato-ku, Tokyo 107
**Department of Physics, Niigata University, Niigata 950-21*
***Faculty of Textile Science and Technology, Shinshu University, Ueda 386*

(Recevied July 20, 1979; Revised July 24, 1980)

By taking the $^{16}O+^{16}O$ system as an example, the property of nucleus-nucleus interaction is investigated by the use of resonating group method. Special attention is paid to the nuclear saturation property which is satisfied in all the interaction region from compact 32-nucleon configuration to two separated ^{16}O nuclei. A new kind of effective nuclear force with a repulsive three-body interaction is introduced in order to take account of density dependent effects in relation to the saturation property. A kind of core in the inner region and a weak attraction in the intermediate region are discussed quantitatively for the $^{16}O+^{16}O$ interaction.

§ 1. Introduction

Experimental systematics on heavy-ion collisions have stimulated the study on nucleus-nucleus interaction.[1)~3)] Theoretical interest has been mainly concentrated upon a potential description by the use of a local density approximation as an intuitive approach.[4),5)] On the other hand, the orthogonality condition model has made a modern current for the study of light two-nucleus systems particularly in Japanese group.[6)] In this model the nucleus-nucleus potential is assumed as some kind of modification of a direct potential. These models, however, are not still placed on a foundation of a fully microscopic consideration on nucleus-nucleus interaction.

Microscopic treatments of the interactions between composite particles have their essential significance in clarifying the interplay of the nuclear force and the Pauli principle during the collision process of two nuclei.[7),8)] Recent progress of the microscopic treatments has rapidly extended their applicability to heavy two-nucleus systems with $(0p)$ or $(1s0d)$ shell nuclei.[9)] An introduction of the generator coordinate[10)] with respect to the relative motion is a key point to succeed in avoiding a serious cumbersomeness in the computational procedures by the use of the resonating group method (RGM). This is because the generator coordinate method (GCM) allows us to utilize the well-known systematics of harmonic oscillator (h.o.) wave function. (And note that when the center-of-mass motion is separated,[11)] the GCM becomes equivalent to the RGM under a Gaussian transfor-

mation.) It is, therefore, possible to study heavy nucleus-nucleus interaction on the basis of the RGM.

In the microscopic study, one of the basic problems is how to choose effective nuclear forces. It was pointed out in a previous paper[12] by studying the $^{16}O+^{16}O$ system that the consideration of nuclear saturation properties plays an essential role in selecting the effective nuclear force; especially the separation energy of ^{16}O from two resonating ^{16}O system as well as that from ^{32}S was necessary to be considered. When the Volkov No. 2 force[13] is adopted, the strength of the Majorana exchange mixture should be taken to be appreciably large for the reproduction of the separation energy. On the other side such an effective nuclear force with simple central terms as the Volkov ones cannot reproduce the empirical binding energy up to heavy nuclei. It is very important for the study of the nucleus-nucleus interaction to overcome these defects in the simple effective nuclear forces. One of the typical attempts is to introduce the density dependent terms in addition to the usual two-body forces. These kinds of effective forces have been known to lead to the success of the Hartree-Fock calculations in the wide mass region of nuclei.[14]

The purpose of this paper is thus to examine the $^{16}O+^{16}O$ interaction by the use of the effective nuclear forces which satisfy the nuclear saturation property in the overall mass region, and to compare the results obtained in the previous studies.[12),21] In this paper the Volkov Nos. 1 and 2 (abbreviated to V1 and V2) are employed as the basis of the two-body force, and the zero-range three-body interaction is introduced as one of the simplest density-dependent terms. The parameters of effective nuclear forces are determined so as to reproduce saturation property of ^{16}O and ^{40}Ca simultaniously such as binding energy and nuclear radius. The compressibility is also taken into consideration. The saturation and binding property of 32-nucleon configuration are studied by examining the binding energy and the separation energies of ^{16}O from ^{32}S and from two resonating ^{16}O nuclei. Whether the evaluated effective nuclear forces are suitable for the relative motion or not is examined through the systematic RGM study of $^{16}O+^{16}O$ configuration.

In § 2, the definitions and formulas about the saturation property are given and the microscopic treatments are recapitulated briefly. The effective nuclear forces are selected by considering the nuclear saturation property in § 3. The calculated results on the $^{16}O+^{16}O$ system are discussed in § 4. Section 5 is devoted to concluding remarks.

§ 2. Theoretical framework and formalism

2.1. *Expressions for saturation property*

First of all, the binding energies of α, ^{16}O, ^{40}Ca and nuclear matter are expressed by using the effective nuclear force with the zero-range three-body interaction which leads to density-dependent effects. The Hamiltonian is defined by

$$H=-\frac{\hbar^2}{2M}\sum_i \nabla_i^2-T_G+\sum_{i<j}(V_{ij}^N+V_{ij}^C)+\sum_{i<j<k}V_{ijk}^{(3)}, \tag{1}$$

where the first term represents the kinetic energy operator, the second comes from the c.m. motion, the third stands for the two-body operator consisting of the nuclear and Coulomb forces and the last term is the three-body interaction. The explicit forms of the third and last terms are written as

$$V_{ij}^N=\sum_k v_k \exp\left(-\left(\frac{r_{ij}}{r_k}\right)^2\right)(w_k+b_kP_\sigma-h_kP_\tau-m_kP_\sigma P_\tau), \tag{2·1}$$

$$V_{ij}^C=\frac{e^2}{r_{ij}}\left(\frac{1+\tau_{zi}}{2}\right)\left(\frac{1+\tau_{zj}}{2}\right) \tag{2·2}$$

and

$$V_{ijk}^{(3)}=v^{(3)}\delta(\boldsymbol{r}_i-\boldsymbol{r}_j)\delta(\boldsymbol{r}_j-\boldsymbol{r}_k), \tag{2·3}$$

where P_σ and P_τ denote the exchange operators on spin and isospin terms, respectively.

By using the h.o. wave function and the Fermi-gas model, total energies per nucleon for α, ^{16}O, ^{40}Ca and nuclear matter are expressed as

$$E_\alpha(a)/A=\frac{9}{16}\hbar\omega+\frac{1}{4}\sum_k v_k\beta_k^{3/2}(X_{dk}+X_{ek})+\frac{1}{4}\left(\frac{2a}{\pi}\right)^{1/2}e^2+\left(\frac{a^2}{3\pi^2}\right)^{3/2}v^{(3)}, \tag{3·1}$$

$$E_O(a)/A=\frac{69}{64}\hbar\omega+\frac{1}{16}\sum v_k\beta_k^{3/2}\left[\left(\frac{31}{4}-\frac{3}{2}\beta_k+\frac{15}{4}\beta_k^2\right)(X_{dk}+X_{ek})+6\beta_k(X_{dk}-X_{ek})\right]+\frac{83}{64}\left(\frac{2a}{\pi}\right)^{1/2}e^2+\frac{29}{9}\left(\frac{a^2}{3\pi^2}\right)^{3/2}v^{(3)}, \tag{3·2}$$

$$E_{Ca}(a)/A=\frac{237}{160}\hbar\omega+\frac{1}{40}\sum v_k\beta_k^{3/2}\left[\left(\frac{1945}{64}-\frac{255}{16}\beta_k+\frac{1455}{32}\beta_k^2-\frac{945}{48}\beta_k^3+\frac{945}{64}\beta_k^4\right)\times(X_{dk}+X_{ek})+\left(\frac{165}{4}\beta_k-\frac{45}{2}\beta_k^2+\frac{105}{4}\beta_k^3\right)(X_{dk}-X_{ek})\right]+\frac{7905}{2560}\left(\frac{2a}{\pi}\right)^{1/2}e^2+\frac{206}{27}\left(\frac{a^2}{3\pi}\right)^{3/2}v^{(3)}, \tag{3·3}$$

$$E_{NM}(k_F)/A=\frac{3}{10}\frac{\hbar^2k_F^2}{M}+\sum_k v_k\left[\frac{(r_kk_F)^3}{24\sqrt{\pi}}X_{dk}+\left\{\frac{1}{4}erf(r_kk_F)+\frac{1}{4\sqrt{\pi}}\frac{1}{(r_kk_F)^3}\times((r_kk_F)^2-2)\exp[-(r_kk_F)^2]+\frac{1}{4\sqrt{\pi}}\frac{1}{(r_kk_F)^3}(3(r_kk_F)^2-2)\right\}X_{ek}\right]+\frac{v^{(3)}k_F^6}{36\pi^4} \tag{3·4}$$

with $X_{dk}=8w_k+4b_k-4h_k-2m_k$, $X_{ek}=8m_k+4h_k-4b_k-2w_k$ and $\beta_k=a/(a+2/r_k^2)$.

Each of Eqs. (3·1)$\sim$(3·4) is arranged in the order of the kinetic, nuclear two-body interaction, Coulomb interaction and zero-range three-body interaction energies. The h.o. size parameter a is related to $\hbar\omega=\hbar^2a/M$ and $\langle r^2\rangle=\{\sum(2n_i+l_i+\frac{3}{2})\}/2aA$. The nuclear incompressibility defined by

$$K=\frac{4a^2}{A}\frac{d^2E(a)}{da^2}\Big|_{a=a_0} \quad \text{and} \quad K=\frac{k_F^2}{A}\frac{d^2E(k_F)}{dk_F^2}\Big|_{k_F=k_{F0}} \tag{4}$$

with a_0 and k_{F0} corresponding to energy minima is also used as a test of the effective nuclear forces. The incompressibility is related to the giant monopole state (GMS) energy by

$$\hbar\Omega=\sqrt{\frac{\hbar^2}{M}\frac{K}{\langle r^2\rangle}}\,. \tag{5}$$

2.2. *The brief presentation of the RGM*

The wave function free from the c.m. coordinate starts with

$$\Psi^{\mathrm{RG}}(1\cdots,32)=\frac{1}{2}\mathcal{A}_{12}\{\phi(^{16}\mathrm{O}_1)\phi(^{16}\mathrm{O}_2)\chi(r)\}, \tag{6}$$

where $\mathcal{A}_{12}$ is the antisymmetrization operator of nucleons between nuclei and $\phi(^{16}\mathrm{O}_i)$ are the internal wave functions of ^{16}O. The relative wave function $\chi(r)$ between two ^{16}O nuclei is expanded into the partial waves: $\chi(r)=\sum_{lm}\{u_l(r)/r\}Y_{lm}(\Omega_r)$. The variational principle of

$$\delta\langle\Psi^{\mathrm{RG}}|H-E|\Psi^{\mathrm{RG}}\rangle=0 \tag{7}$$

leads to the well-known integro-differential RGM equation with respect to the radial part of the relative wave function:

$$\int\{H_l(r,r')-EN_l(r,r')\}u_l(r')dr'=0\,. \tag{8}$$

Here $H_l(r,r')$ and $N_l(r,r')$ are the energy and normalization kernels which are defined by

$$H_l(r,r')=\left\{-\frac{\hbar^2}{2\mu}\left(\frac{d^2}{dr^2}-\frac{l(l+1)}{r^2}\right)+V_D(r)\right\}\delta(r-r')-K_l^H(r,r'), \tag{9·1}$$

$$N_l(r,r')=\delta(r-r')-K_l^N(r,r'), \tag{9·2}$$

where μ is the reduced mass and $V_D(r)$ represents the direct (folding) potential which is obtained by removing the antisymmetrizer and by operating two- and three-body terms in the Hamiltonian. A straightforward calculation gives the direct potential:

$$V_D(r)=2\sum_k\left\{X_{dk}v_k\gamma_k^{3/2}\exp[-\gamma_k(r/r_k)^2]\right.$$

$$\times\left[16-\frac{16\gamma_k}{ar_k^2}\left(1+\frac{\gamma_k}{2}\right)+\frac{16\gamma_k^2}{3ar_k^4}(1+2\gamma_k)r^2+\frac{4\gamma_k^4}{a^2r_k^8}r^4\right]\Bigg\}$$
$$+\frac{(8e)^2}{r}\left[erf\left(\sqrt{\frac{8}{15}}ar\right)-\left(\frac{8}{15}\right)^{5/2}\left(\frac{3}{2}+\frac{2}{15}ar^2\right)r\sqrt{\frac{a}{\pi}}\exp\left(-\frac{8}{15}ar^2\right)\right]$$
$$+\frac{64}{11^3}\left(\frac{a^2}{3\pi^2}\right)^{3/2}v^{(3)}\left[16187+\frac{2^5\cdot3\cdot593}{11}ar^2+\frac{2^{13}\cdot23}{11^2}a^2r^4\right.$$
$$\left.+\frac{2^{17}}{11^3}a^3r^6\right]\exp\left(-\frac{8}{11}ar^2\right) \tag{10}$$

with $\gamma_k=8a/(8a+15/r_k^2)$. The Coulomb interaction and three-body interaction kernels are correctly evaluated through an analytical derivation in computational way as well as the Gaussian type two-body interaction one.[22] A new method of a systematic calculation of all the energy kernels will be reported elsewhere by one of the present authors (A. T-S.).

The RGM equation (8) is solved by means of Mito and Kamimura's method[15] which is developed on the basis of the Kohn-Hulthen-Kato variational method.[16] By using an approximate trial wave function $u_l^t(r)$, the variational principle is applied to a functional

$$J[u_l^t]=S_l^t+i\frac{k\hbar^2}{\mu}\int_0^\infty\int_0^\infty u_l^t(r)\,[H_l(r,r')-EN_l(s,r')]\,u_l^t(r')\,drdr'. \tag{11}$$

A stationary solution obtained from the variation $\delta J(u^{st})=0$ is a solution of Eq. (8). The S-matrix S_l under a proper boundary condition of scattering states is obtained by $S_l\simeq J[u_l^{st}]$, which is an approximate solution within the error of the second order (see Ref. 15)). The linear combination of the Gaussian wave packets around R_i plus the Coulomb wave function modified in the interial region is employed as a trial wave function. When the Gaussian wave packets with an appropriate size parameter are adopted, the matrix element of the RGM kernel between two wave packets is just in agreement with the GCM kernel itself. In this sense, the RGM kernel whose calculation is very difficult for heavy two-nucleus system is replaced by the GCM one.

§ 3. Nuclear saturation property and effective nuclear forces

The aim of this section is to adjust the parameters of the effective nuclear forces (2·1)$\sim$(2·3) so that they become appropriate to the study of the interaction between $(0p)$-shell nuclei. Table I summarizes the parameters. For reference the Brink-Boeker No. 1[17] (BB1) force will be also used in view of its extremely strong Majorana exchange character. Calculated binding energy, rms radius, incompressibility and GMS energy are exhibited in Table II for α, ^{16}O, ^{40}Ca and nuclear matter.

Table I. Parameters of the effective nuclear forces to be used.

Force	r_k(fm)	V_k (MeV)	w_k	m_k	b_k	h_k	$v^{(3)}$ (MeV·fm^6)
V2(0.65)	1.80	−60.65	0.350	0.650	0.0	0.0	0
	1.01	61.14					
MV2 case 1	1.80	−60.65	0.382	0.618	0.0	0.0	4000
	1.01	40.14					
MV2 case 2	1.80	−60.65	0.382	0.618	0.0	0.0	4000
	1.01	38.14					
MV1 case 1	1.60	−83.34	0.400	0.600	0.0	0.0	5000
	0.82	99.86					
MV1 case 2	1.60	−83.34	0.400	0.600	0.0	0.0	5000
	0.82	96.86					
MV1 case 3	1.60	−83.34	0.400	0.600	0.0	0.0	4000
	0.82	104.86					
BB1	1.40	−140.6	0.5136	0.4864	0.0	0.0	0
	0.70	389.5	1.529	−0.529	0.0	0.0	

Table II. Physical quantities on saturation property and incompressibility and monopole energy.

	Force	V2(0.65)	MV2 case 1	MV2 case 2	MV1 case 1	MV1 case 2	MV1 case 3	BB1	exp.
α	E/A (MeV)	6.99	7.16	7.38	7.04	7.24	7.19	6.85	7.08
	$\hbar\omega$ (MeV)	21.77	17.42	17.62	17.42	17.24	18.04	20.73	
	rms (fm)	1.69	1.89	1.88	1.89	1.89	1.86	1.73	1.61
	K (MeV)	78.94	88.13	90.43	99.26	99.06	96.27	76.97	
	$\hbar\Omega$ (MeV)	26.64	31.99	32.60	33.95	33.92	34.03	32.62	
^{16}O	E/A (MeV)	6.62	7.64	7.92	7.64	7.90	7.89	5.81	7.93
	$\hbar\omega$ (MeV)	16.17	13.06	13.27	13.06	13.27	13.89	13.06	
	rms (fm)	2.40	2.67	2.65	2.67	2.65	2.59	2.67	2.64
	K (MeV)	60.11	103.88	107.79	117.36	122.04	120.31	92.77	
	$\hbar\Omega$ (MeV)	20.79	24.56	25.21	26.10	26.83	27.26	23.21	∼26.4
^{40}Ca	E/A (MeV)	8.70	8.99	9.34	8.79	9.10	9.27	6.27	8.55
	$\hbar\omega$ (MeV)	17.62	11.40	11.61	11.20	11.20	11.82	10.57	
	rms (fm)	2.66	3.30	3.27	3.33	3.33	3.24	3.43	3.52
	K (MeV)	63.33	129.92	136.03	145.33	144.99	142.82	102.54	
	$\hbar\Omega$ (MeV)	19.29	22.22	22.95	23.29	23.26	23.72	19.01	∼23.5
N.M.	E/A (MeV)	—	24.34	25.12	21.01	21.61	23.50	15.69	15.64
	k_f (fm^{-1})	—	1.59	1.60	1.48	1.49	1.57	1.45	1.36
	K (MeV)	—	333.01	346.60	299.29	311.57	325.50	184.41	

Let us note V2(0.65) for example. It can reproduce the separation energies of ^{16}O from ^{32}S and from two resonating ^{16}O configuration,[12] however, serious defects are that

(i) the binding energy of ^{16}O is not reproduced,

(ii) the rms radius of ^{40}Ca is too small in comparison with the empirical value,

(iii) the GMS energies $\hbar\Omega$ for ^{16}O and ^{40}Ca are appreciably smaller than $2\hbar\omega$ indicated by the empirical $\sim 80/A^{1/3}$ law,

(iv) the energy of nuclear matter does not have minimum up to $k_F = 3fm^{-1}$.

The zero-range three-body interaction $v^{(3)}$ of Eq. (2·3) has been introduced to overcome these defects. The strength of $v^{(3)}$ is determined by paying attention to the binding energy of ^{16}O. The strength of $v^{(3)}$ and the short range repulsion in the two-body interaction are balanced*) so as to reproduce the binding energy of ^{16}O. The MV2 and MV1 versions in Table I are modified from Volkov No. 2 ans No. 1, respectively. The introduction of the repulsive $v^{(3)}$ adjusted to ^{16}O leads to the following trends:

(i) The binding energies of ^{40}Ca and nuclear matter approach empirical values only with larger strength of $v^{(3)}$, but the energy of α is not so deviated from the experiments.

(ii) The rms radius of all the nuclei and the incompressibility of ^{16}O and ^{40}Ca are in good agreement with experiments.

The deviation calculated from empirical total energy expressed in terms of $(E_{\text{cal}} - E_{\text{exp}})/E_{\text{exp}}$ is shown versus mass number A in Fig. 1. The energy of nuclear matter considerably depends upon the strength $v^{(3)}$. The cases labeled as a correspond to the strength $v^{(3)} = 4000$ MeV fm^6 while the cases with label b to $v^{(3)} = 5000$ MeV fm^6. If the binding energy of ^{16}O is almost exactly adjusted, that of ^{40}Ca becomes somewhat too large. Two types, therefore, are searched; the first one generates a slight lack of the binding energy of ^{16}O and a slight excess for ^{40}Ca (denoted by group 1) and the second one reproduces the binding energy of ^{16}O at the expense of ^{40}Ca (group 2). In the mass region between ^{16}O and ^{40}Ca the MV2 case 1 and MV1 case 1 show a common trend in Fig. 1, constituting group 1, while the MV2 case 2 and MV1 case 2 and 3 belong to the group 2. The BB1 force shows a serious defect that neither binding energy of ^{16}O nor that of ^{40}Ca can be reproduced.

Let us next consider the mutual relation of the separation energies of ^{16}O from ^{32}S and from two resonating ^{16}O configuration. Two kinds of separation energies are introduced as

$$\delta E_0 = (-E_0^{\text{S}}(a_{\text{s}})) - (-2E^{\text{O}}(a_{\text{o}})) \qquad (12\cdot1)$$

and

*) This procedure was first proposed by Yamamoto[19] on the basis of Hasegawa-Nagata force.[20]

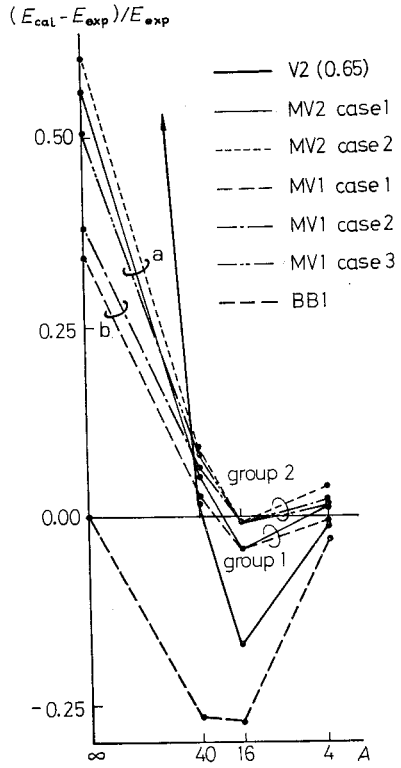

Fig. 1. Energy deviation of the calculated total energy from the empirical one, which is expressed by $(E_{cal}-E_{exp})/E_{exp}$. Circle a means the force with $v^{(3)}=4000$ MeV fm^6 and circle b corresponds to the case with $v^{(3)}=5000$ MeV fm^6.

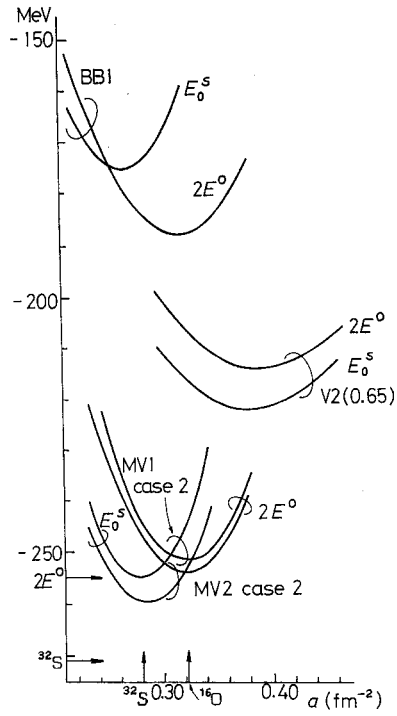

Fig. 2. Total energy curves with respect to a for ^{32}S and $2E^O$.

$$\Delta E_0=(-E_0^{O+O}(a_o))-(-2E^O(a_o)), \qquad (12\cdot2)$$

where E_0^S is the energy of the ^{32}S ground state*) and E_0^O is the energy of ^{16}O with $(0s)^4(0p)^{12}$ configuration. The energy E^{O+O} is the minimum value of the RGM equation (8), namely, the energy of two resonating ^{16}O nuclei. The size parameters a_o and a_s are those for the energy minima of ^{16}O and ^{32}S, respectively. The empirical separation energy is referred to

$$\delta E_{exp}=B(^{32}S)-2B(^{16}O). \quad (=16.54\,\text{MeV}) \qquad (13)$$

Let us impose the following two conditions which give criteria to select the forces

*) The ground state $(1s0d)^{16}$ configuration is assumed to be $\{(1s0d)^{16}[4444]\,(\lambda\mu)=(48), K^\pi=0^+\}$ which is practically constructed by α-cluster model as mentioned in the Appendix of Ref. 12).

appropriate for the study of the relative motion between complex nuclei. The first one is

$$\Delta E_0 \lesssim \delta E_{\text{exp}}\,, \tag{14}$$

which means that two resonating ^{16}O configuraton should belong to an excited state of ^{32}S nucleus. The second one is that calculated binding energy of ^{32}S should be larger than that of the two resonating ^{16}O configuration; that is,

$$\Delta E_0 \lesssim \delta E_0 \tag{15}$$

which describes a consistent result for the energy relation within the framework of the model calculation.

For the pure two-body central force, say V2 case, the Majorana strength m has to be around 0.65 in order to satisfy these two conditions. However, the size parameters conflict with empirical ones as seen in Fig. 2; namely, a_o becomes even smaller than a_s in addition that both a_o and a_s are too large. This serious defect clearly implies the inadequency of V2 type simple effective forces.

Calculated energy surfaces are shown in Fig. 2 for all the forces presently deviced. Table III summarizes relevant calculated quantities. It is clear from Fig. 2 and Table III that all the new forces not only satisfy the above conditions but also reproduce quite well the empirical binding energies and rms radii of ^{16}O and ^{32}S nuclei. In Fig. 2, the arrows on the axis of ordinate indicate the empirical size parameters a for ^{16}O and ^{32}S while those on the axis of abscissas do the empirical binding energies for two ^{16}O and ^{32}S. Note that the BB1 case conflicts with condition (15), too. Significant improvement achieved by our new forces is entirely due to the introduction of the three-body interaction. This point will be essential in studying the interaction between composite particles. It is thus considered that BB1 force used in detailed calculations of ^{16}O+^{16}O interaction by Brussel group[21] is not suited for the study of two-nucleus system in $(0p)$ and $(1s0d)$ shell mass

Table III. The energy quantities to consider the mutual relation of separation energy of ^{16}O from ^{32}S and two resonating ^{16}O system.

(Unit in MeV)

Force	E_0^S	$\hbar\omega_s$	$2E^o$	E_0^{RGM}	$\hbar\omega_o$	ΔE_0	δE_0
V2(0.65)	−219.7	15.8	−211.8	−215.8	16.2	4.0	7.9
MV2 case 1	−250.4	11.6	−244.3	−246.3	13.1	2.0	6.1
MV2 case 2	−260.6	11.6	−253.5	−256.1	13.3	2.6	7.1
MV1 case 1	−246.7	11.6	−244.6	−243.6	13.1	−1.0	2.1
MV1 case 2	−255.8	11.6	−252.7	−252.1	13.3	−0.6	3.1
MV1 case 3	−258.0	12.0	−252.6	−253.3	13.9	0.7	5.4
BB1	−172.3	10.8	−186.0	−179.2	13.1	−6.8	−13.7
Exp.	−271.7		−255.2				16.5

region.

§ 4. $^{16}O+^{16}O$ interaction by the RGM

4.1. *Phase shifts and energy spectra*

In Fig. 3 calculated phase shifts are shown for the MV2 case 2 and MV1 case 1 forces in comparison with V2(0.65) and BB1. The phase shifts for all the MV2 forces show a similar behavior and those for all the MV1 resemble each other. The bound and resonance state energy spectra are exhibited versus $l(l+1)$ in Figs. 4(a) and (b) for group 1 and 2 forces, respectively. The BB1 and V2(0.65) cases are shown for reference.

Figures 4(a) and (b) indicate two pure rotational bands satisfying the $l(l+1)$ rule for all the cases except for BB1. The character of the bands is arranged in terms of the band head energy and the rotational constant $k=\hbar^2/2\mathcal{J}$ in Table IV. The width of the resonances increases with increasing l and the width of $l=18$ on the second band becomes about 2.5 MeV for all the new forces.

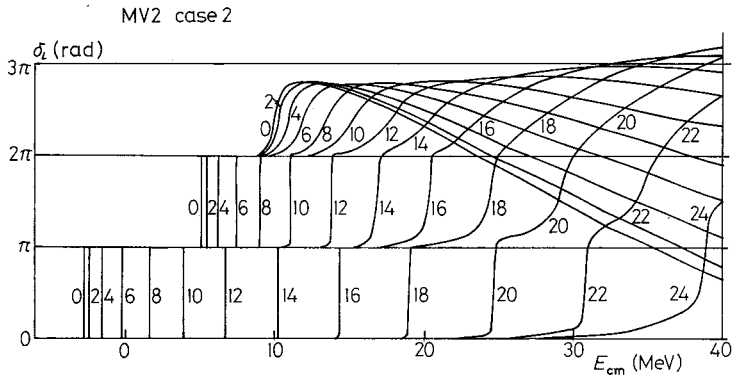

(a)

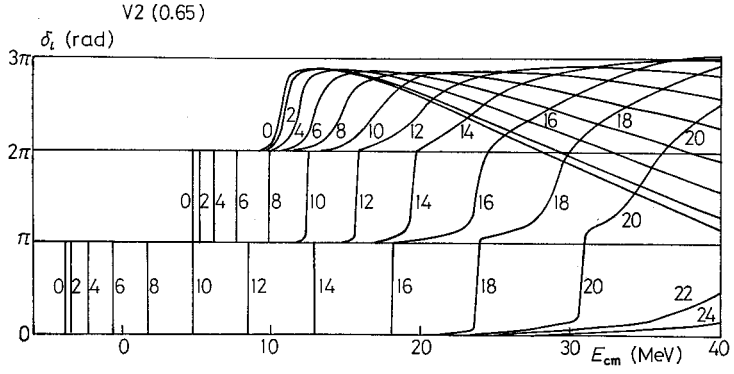

(b)

Fig. 3. (Continued)

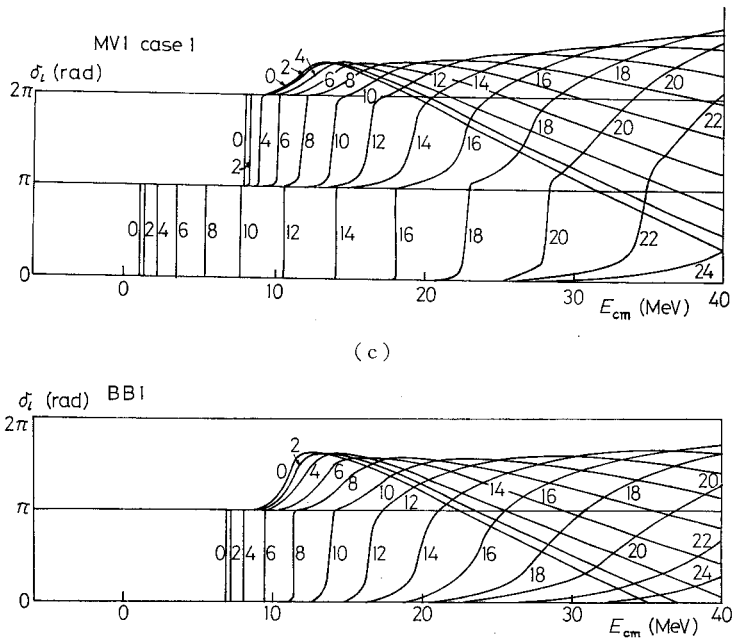

Fig. 3. Phase shifts.

Table IV. The properties of the rotational bands for the $^{16}O+^{16}O$ system.

Force	No. of band	E_0 (MeV)	$K=\hbar^2/2\mathcal{J}$ (keV)
V2(0.65)	1st	−3.9	89
	2nd	4.8	70
MV2 case 1	1st	−1.9	60
	2nd	5.7	56
MV2 case 2	1st	−2.7	64
	2nd	5.2	56
MV1 case 1	1st	1.0	63
	2nd	7.9	54
MV1 case 2	1st	0.5	65
	2nd	7.7	55
MV1 case 3	1st	−0.7	66
	2nd	6.9	58
BB1	1st	6.8	62

The band head energy depends upon whether the force is MVI or MV2 rather than whether it belongs to group 1 or 2. The energy for MV1 is higher than that for MV2 by 2∼3 MeV. In the energy range $E_{cm}=20\sim30$ MeV where three prominent gross structures are observed,[23] the resonance energies on the second band correspond to $l=16$, 18 and 20 for new forces. Considering the energy

spacing and the energy region, the resonant partial waves $l=16$, 18 and 20 on the second band for new forces are expected to play a major role in the gross structure. On the other hand, the partial waves $l=14$, 16 and 18 are appropriate to representation of the gross structure if V2(0.65) is adopted. This comes from smaller moment of inertia than the others.

In all the cases of new forces the rotational constant k is about 63 keV for the first band, while it becomes smaller by about 7 keV for the second band. The

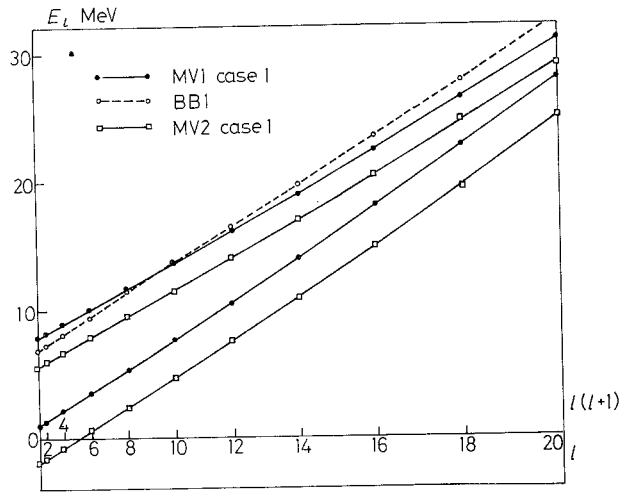

(a)

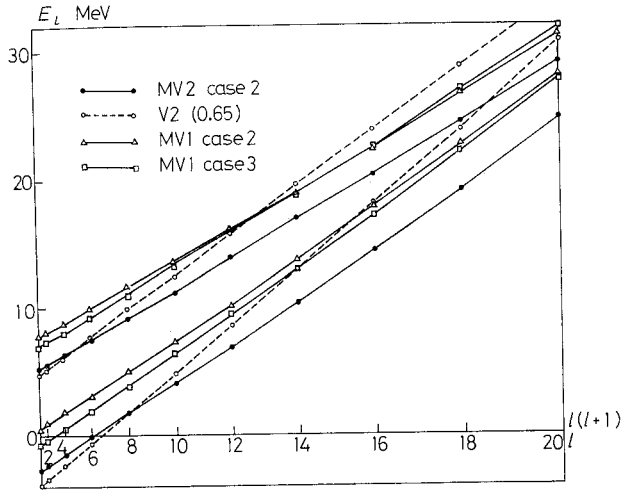

(b)

Fig. 4. (a) Energy spectra of bound and resonant states for the forces belonging to group 1. (b) Energy spectra of bound and resonant states for the forces belonging to group 2.

energy splitting between two bands, therefore, decreases with increasing angular momentum. The rotational constants for two bands in V2(0.65) case are 89 keV and 70 keV, respectively, reflecting larger separation of two ^{16}O. The BB1 force generates only one rotational band whose moment of inertia resembles that of the first band for the others, but the resonance widths become wide for high angular momentum ($\Gamma=3.2$ MeV for $l=18$, for instance). As far as the adopted effective nuclear forces which satisfy the saturation property, the rotational constant k is almost independent of the forces.

4.2. *Energy curves*

In Fig. 5 are shown the energy curves defined by subtracting $2E^{O}$ from the total energy with respect to the relative distance R. The characteristics do not depend upon the group of forces but upon either MV1 or MV2.

For all the new forces and V2(0.65) the energy curves have local minima up

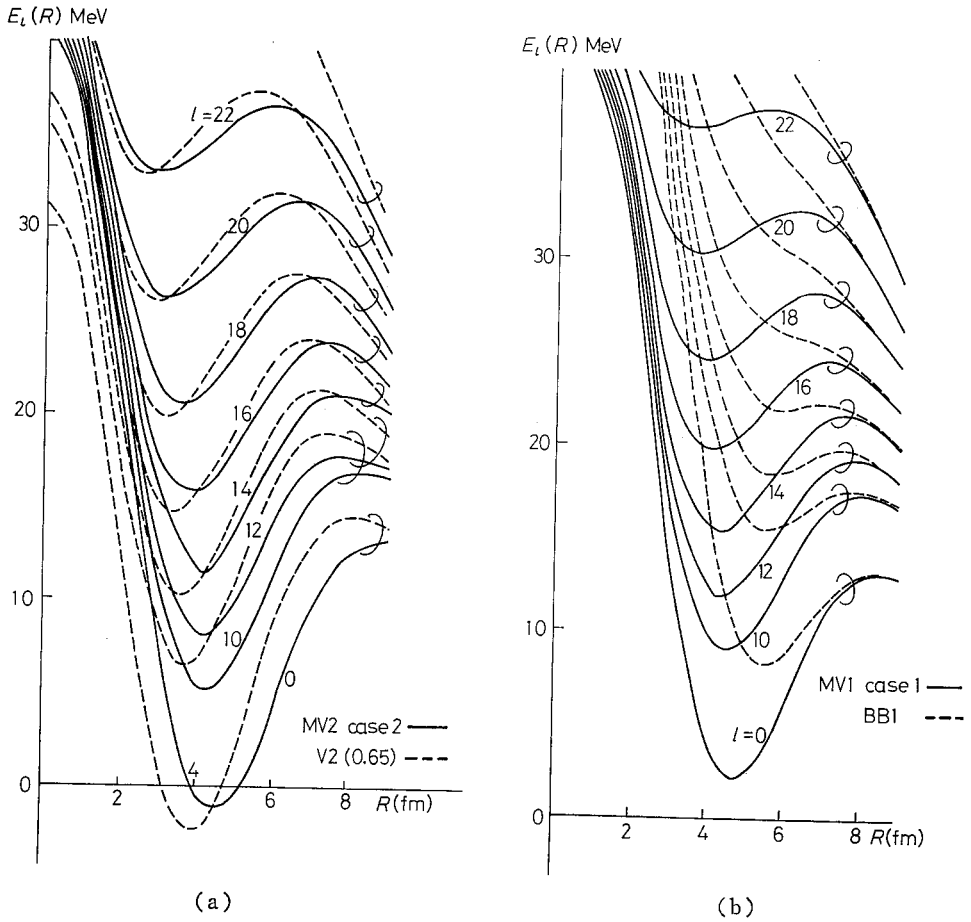

Fig. 5. Energy surfaces with respect to the relative distance parameter R.

to $l=24$ around $R=3\sim5$ fm. The minimum point decreases with the increase of angular momentum l because of an antistretching effect mainly due to the Pauli principle. However, this point R does not directly correspond to the rms distance ($\sqrt{\langle r^2\rangle}$) of the relative wave function but the actual rms distance is almost constant up to $l=24$.

Let us next compare the MV2 case 2 with V2(0.65) forces which almost reproduce the empirical separation energy of ^{16}O from ^{32}S. The energy curve for MV2 case 2 is lower at larger R and higher at smaller R than that for V2(0.65). In the inner region the density-dependent effects due to $v^{(3)}$ push up the energy curve of MV2 case 2 while in the outer region the weak Majorana force presses it down. In other words, the three-body interaction prevents a compact 32-nucleon system from high nuclear density in the overlapping region, while the strong Majorana force lifts up the total energy in all the region. The densiy dependence, therefore, pushes out the minimum point of the energy curve toward the contact distance. This is responsible for the rotational constant k smaller for MV2 case

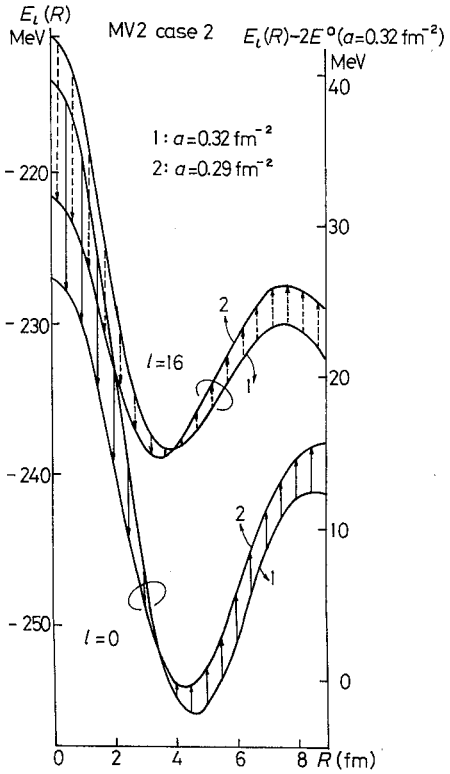

Fig. 6. Energy surface to see the behavior of the size parameter a.

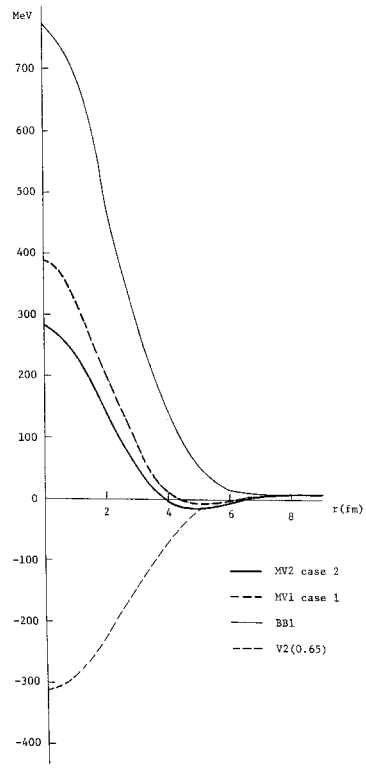

Fig. 7. Direct potentials $V_D(r)$.

2. This tendency persists for all the new forces satisfying the saturation property of $(0p)$ and $(1s0d)$ shell nuclei. The BB1 force, which conflicts with the condition (15) (see Fig. 2(g)), makes a shallow pocket for the lower l but no longer makes any pocket beyond $l=16$.

At the end of this subsection, size parameter dependence in MV2 case 2 is examined in all the interaction region. In Fig. 6 energy curves for $a=0.32\,\mathrm{fm}^{-2}$ and $0.29\,\mathrm{fm}^{-2}$ and for $l=0$ and 16 are demonstrated. The case with $a=0.32\,\mathrm{fm}^{-2}$ reproduces the binding energy of ^{16}O, while the case around $a=0.29\,\mathrm{fm}^{-2}$ leads to the energy minimum of the configuration $SU_3(24,0)$. (Note that $SU_3(24,0)$ wave function is given by the limit $R\to 0$.) The energy curve for $a=0.32\,\mathrm{fm}^{-2}$ is higher in the inner region but lower in the outer region. The arrowed and dashed lines at a fixed R show energy change for $l=0$ and 16, which mainly comes from the role of the strong incompressibility. For $l=0$ the energy minimum of the case with $a=0.32\,\mathrm{fm}^{-2}$ is lower than the other by 2 MeV, while for $l=16$ the two energy minima approach each other. This result is interesting, since higher l than 14 may play an important role in gross structure phenomena observed in the excitation function.

4.3. *Direct potential and effective potential*

Direct potentials calculated by Eq. (10) are shown in Fig. 7. The new forces show a repulsive core in the inner region and a weak attraction of $\sim$15 MeV in the intermediate region. On the other side, the direct potential of BB1 has no pocket in all the regions reflecting its extremely strong exchange character. As is known the V2(0.65) case leads to a deep attractive well.

Let us see the roles of the three-body interaction by taking MV2 case 2 as an example. Figure 8 demonstrates divided contributions to the direct potential. The contribution of the three-body interaction rapidly falls down and disappears at the contact distance of about 6 fm. On the other hand, the nuclear two-body interaction remains important up to 9 fm. A weak attraction of the direct potential originates in this deviation.

An effective local potential is defined by

$$V^l_{\mathrm{eff}}(r)=\left[\left\{E_{\mathrm{cm}}-\left(\frac{\hbar^2}{2\mu}\right)\left(\frac{d^2}{dr^2}-\frac{l(l+1)}{r^2}\right)\right\}\psi_l(r)\right]/\psi_l(r), \tag{16}$$

where the wave function $\psi_l(r)$ free from redundancy is given by $\psi_l=\sqrt{1-\hat{K}_l{}^N}u_l$ with a usual normalization $\langle\psi_l|\psi_l\rangle=1$.[24] This potential is studied on the first band for the evaluated new forces. In Fig. 9, the effective local potentials for $l=0$ and 16 of the first band are shown for MV2 case 2 and V2(0.65) forces. It is assumed by following the investigation of $\alpha+\alpha$[7] that the "structural one" is generated at the outermost nodal point of the inner oscillation. The character of the effective local potential in the intermediate region is shown not only in an attrac-

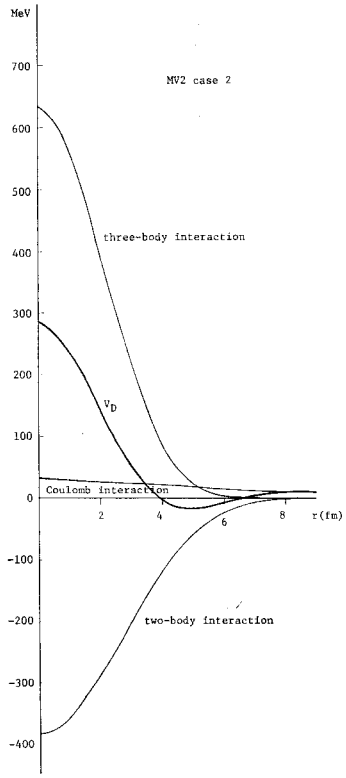

Fig. 8. Direct potential $V_D(r)$ divided into three terms, nuclear two-body, Coulomb and three-body interaction ones.

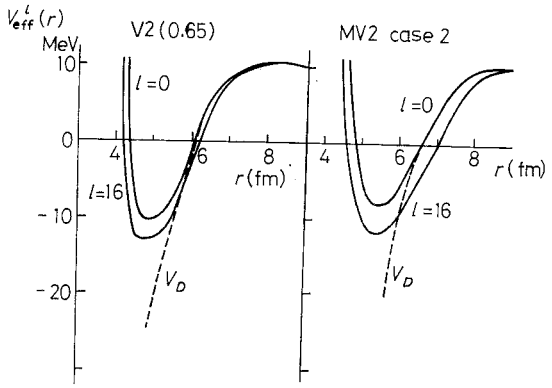

Fig. 9. Effective local potentials, where dashed curves denote the direct potential.

tion of 10 MeV for $l=0$ but also in a behavior like an l-dependent potential.*)

In the outer region the effective local potential is described by the direct potential plus a weak repulsion due to a few particle exchange effects. The MV2 case 2 pushes out the minimum point by 0.5 fm from that of V2(0.65). The effective potential diverges at the nodal points of the wave function because the zero point of the denominator of Eq. (21) does not agree with that of the numerator. This is due to the non-locality of the kernels in the RGM equation. In this sense, the energy and angular momentum dependences of local potential in the wide energy region cannot be discussed at the present stage. In the near future, however, this point will be investigated in a wide field on the nucleus-nucleus interaction.

*) In the previous paper,[12] a stronger l-dependency than the present case was illustrated, where the Coulomb interaction kernel was approximated by the direct part of it. In the present work, however, it is treated exactly. This difference is produced by the exact treatment of it.

§ 5. Concluding remarks

On the basis of Volkov type forces, proposed are new kinds of effective nuclear forces responsible for the study of relative motion, which reproduce the nuclear saturation property in the wide range of nuclei, especially in the region from ^{16}O to ^{40}Ca. It is indicated that the BB1 force has a serious defect about the binding energy of nuclei of this region, and that the V2(0.65) cannot also reproduce the empirical nuclear size and incompressibility. The new forces succeed in overcoming these defects on the saturation property. The introduction of density-dependent effect as three-body interaction is one of the essential points to satisfy the empirical saturation property and incompressibility of nuclei simultaneously. These forces also succeed in leading to correcting separation energies of ^{16}O from ^{32}S and from two resonating ^{16}O configuration.

In a manner similar to our previous papers,[12),25)] the interaction of the $^{16}O+^{16}O$ system is summarized by dividing the interaction region into three:

(i) In the inner region the concept of "core" potential is confirmed to be valid. This "core" potential is strengthened by the strong incompressibility of nuclei for the present new forces. It is pointed out by the energy height at origin ($R=0$) as seen in Fig. 5 and also by seeing the behavior of the wave functions that the core may be melted above $E_{cm}\sim 50$ MeV.

(ii) There appears the attractive ability in the intermediate region which produces two pure rotational bands. There is no essential difference between the present result and the previous one of V2(0.65). It is also pointed out that even if the nuclear saturation property is satisfied in all the region of mass number, the character in the intermediate region depends upon the detialed property of the effective nuclear force.

(iii) The outer region may be represented by the direct potential plus a weak repulsion when such a force with moderate exchange mixture as the Volkov one is employed.

The new forces are a kind of the effective nuclear force inducing cluster structure and favouring molecular formation in the following meanings:

(i) The density-dependent effect as the repulsive three-body interaction in the inner region prevents two separated nuclei from their dissolution.

(ii) An attractive two-body interaction with a finite range makes two nuclei combine in the interaction region.

These characteristics of the forces and the role of the Pauli principle may give a theoretical basis of the occurrence of "quasi-molecular resonances".[26)] It will be of more interest that the experimental data are analyzed by the use of new forces within the framework of the microscopic model with the introduction of a phenomenological imaginary potential.

Acknowledgements

A part of this work is the doctor thesis of one of the authors (T.A.) at Hokkaido University. He would like to express his gratitude to Professor H. Tanaka and Professor Y. Akaishi and the members of the laboratory of nuclear theory for their interst and encouragment. This work was performed as a part of the annual research project on the "Highly Excited States in Nuclei and Molecular Resonances", organized by the Research Institute for Fundamental Physics, Kyoto University, 1976~1978. The authors thank all the members of this project, particularly Dr. T. Matsuse for fruitful discussions. They are indebted to Dr. M. Kamimura for his coorperative cosideration in utilizing the computational code VAR-GCM to solve the RGM equation. They are also grateful to Professor R. Tamagaki, Professor H. Bandō and Dr. Y. Yamamoto for their continuous encouragement and discussions especially on the effective nuclear force. Two of the authors (T.A. and K.I.) thank the members of nuclear laborratory at Niigata University for their encouragement and discussions. The computational work was performed at the Computer Center of University of Tokyo.

References

1) *Proceedings of the International Conference on Cluster Aspects of Nuclear Structure and Nuclear Reactions, Winnipeg, 1978.*
2) *Proceedings of the International Symposium on Nuclear Collisions and Their Microscopic Description, Bled,* Fizika **9** suppl. (1977).
3) *Proceedings of the International Conference on Resonances in Heavy Ion Reactions, Hvar, 1977.*
4) K. A. Brueckner, J. R. Buchler, S. Jorna and R. J. Lombard, Phys. Rev. **171** (1968), 1188.
   K. A. Brueckner, J. R. Buchler, R. C. Clark and R. J. Lombard, Phys. Rev. **181** (1969), 1543.
5) G. Negô, B. Tamalin, J. Galin, M. Beiner and R. J. Lombard, Nucl. Phys. **A240** (1975), 353.
   D. M. Brink and FL. Stancu, Nucl. Phys. **A243** (1975), 175.
   FL. Stancu and D. M. Brink, Nucl. Phys. **A270** (1976), 236.
6) S. Saito, Prog. Theor. Phys. **40** (1968), 893; **41** (1969), 705.
   T. Matsuse and M. Kamimura, Prog. Theor. Phys. **49** (1973), 1765.
   Y. Suzuki, Prog. Theor. Phys. **55** (1976), 1751; **56** (1976), 111.
7) K. Wildermuth and T. V. Kanellopoulous, Nucl. Phys. **7** (1958), 150.
   R. Tamagaki and H. Tanaka, Prog. Theor. Phys. **34** (1965), 191.
   S. Okai and S. C. Park, Phys. Rev. **145** (1966), 787.
8) W. Sünkel and K. Wildermuth, Phys. Letters **41B** (1972), 439.
   T. Matsuse, M. Kamimura and Y. Fukushima, Prog. Theor. Phys. **53** (1975), 706.
9) K. Ikeda, R. Tamagaki, S. Saito, H. Horiuchi, A. Tohsaki-Suzuki and M. Kamimura, Prog. Theor. Phys. Suppl. No. 62 (1977).
10) H. Horiuchi, Prog. Theor. Phys. **43** (1970), 375.
11) A. Tohsaki-Suzuki, Prog. Theor. Phys. **59** (1978), 1261.
12) T. Ando, K. Ikeda and A. Tohsaki-Suzuki, Prog. Theor. Phys. **61** (1979), 101.
13) A. B. Volkov, Nucl. Phys. **74** (1965), 33.
14) For instance, T. H. R. Skyrme, Nucl. Phys. **9** (1959), 615.
   D. Vantherin and D. M. Brink, Phys. Rev. **C5** (1972), 626.

15) Y. Mito and M. Kamimura, Prog. Theor. Phys. **56** (1976), 583.
M. Kamimura, Prog. Theor. Phys. Suppl. No. 62 (1977), 236.
16) W. Kohn, Phys. Rev. **74** (1948), 1973.
L. Hulthen, Ark. Mat. Astr. Fys. **35A** (1948), No. 25.
T. Kato, Prog. Theor. Phys. **6** (1951), 295, 394.
17) D. M. Brink and E. Boeker, Nucl. Phys. **B91** (1967), 1.
18) For experiments,
D. R. Brown and J. D. Bronson, Phys. Rev. Letters **39** (1977), 1188.
S. Sasano and Y. Torizuka, Phys. Rev. **C15** (1977), 217.
For theory,
K. Ando and M. Kohno, Prog. Theor. Phys. **60** (1978), 304.
M. Kohno and K. Ando, Prog. Theor. Phys. **61** (1979), 1065.
19) Y. Yamamoto, private communication.
20) A. Hasegawa and S. Nagata, Prog. Theor. Phys. **45** (1971), 1786.
21) D. Baye and G. Reidemeister, Nucl. Phys. **A258** (1976), 157.
D. Baye and P.-H. Heenen, Nucl. Phys. **A276** (1977), 354.
22) A. Tohsaki-Suzuki, Prog. Theor. Phys. Suppl. No. 62 (1977), 191.
23) J. V. Maher, M. W. Sachs, R. H. Siemssen, A. Weidinger and D. A. Bromley, Phys. Rev. **188** (1669), 1665.
A. Gobbi, R. Wieland, L. Chuwa, D. Shapira and D. A. Bromley, Phys. Rev. **C7** (1973), 30.
24) S. Saito, S. Okai, R. Tamagaki and M. Yasuno, Prog. Theor. Phys. **50** (1973), 1561.
25) A. Tohsaki, F. Tanabe and R. Tamagaki, Prog. Theor. Phys. **53** (1975), 1022.
T. Ando, K. Ikeda and Y. Suzuki Prog. Theor. Phys. **54** (1975), 119.
26) E. Almqvist, D. A. Bromley and J. A. Kuehner, Phys. Rev. Letters **4** (1960), 515.
E. Almqvist, D. A. Bromeley, J. A. Kuehner and B. Wahlen, Phys. Rev. **130** (1963), 1140.